Entanglement of Nambu Spinors and Bell Inequality Test without Beam Splitters

Wei Luo,[1,2] Hao Geng,[1] D. Y. Xing,[1] G. Blatter,[3] and Wei Chen[1,3,*]
[1]*National Laboratory of Solid State Microstructures, School of Physics, and Collaborative Innovation Center of Advanced Microstructures, Nanjing University, Nanjing 210093, China*
[2]*School of Science, Jiangxi University of Science and Technology, Ganzhou 341000, China*
[3]*Institute for Theoretical Physics, ETH Zurich, 8093 Zurich, Switzerland*

(Received 30 September 2021; accepted 6 September 2022; published 16 September 2022)

The identification of electronic entanglement in solids remains elusive so far, which is owed to the difficulty of implementing spinor-selective beam splitters with tunable polarization direction. Here, we propose to overcome this obstacle by producing and detecting a particular type of entanglement encoded in the Nambu spinor or electron-hole components of quasiparticles excited in quantum Hall edge states. Because of the opposite charge of electrons and holes, the detection of the Nambu spinor translates into a charge-current measurement, which eliminates the need for beam splitters and assures a high detection rate. Conveniently, the spinor correlation function at fixed effective polarizations derives from a single current-noise measurement, with the polarization directions of the detector easily adjusted by coupling the edge states to a voltage gate and a superconductor, both having been realized in experiments. We show that the violation of Bell inequality occurs in a large parameter region. Our Letter opens a new route for probing quasiparticle entanglement in solid-state physics exempt from traditional beam splitters.

DOI: 10.1103/PhysRevLett.129.120507

Appearing as a mystery in the early days of quantum mechanics [1,2], quantum entanglement has become a central resource of modern quantum information science [3,4], which results in important applications in quantum computation, communication, and other protocols [5,6]. Despite its ubiquity in quantum many-body systems, producing and manipulating entanglement in a controllable way requires great effort. In practice, entangled states can be carried by different particles and various physical degrees of freedom, which has stimulated diverse explorations in different branches of physics. In particular, the manipulation of entangled photons has turned into a mature technology [7]; by contrast, the detection of entanglement between quasiparticles in solids remains a challenge.

As an electronic analog of quantum optics, various quantum interference effects have been implemented in mesoscopic transport experiments [8–12]. With this inspiration, numerous theoretical proposals have been made to generate and detect spin and orbital entanglement between separated electrons, or more precisely, quasiparticles, in solid-state physics [13–28]. Experimental progress has also been made in the entanglement production via Cooper pair splitting in hybrid superconducting structures [29–37]. Nevertheless, the verification of the expected entanglement remains out of reach, and further development in this direction has been rather scarce in the past decade. The main obstacle hindering the detection of spin and orbital entanglement is the demand for high-quality spinor-selective beam splitters [15–26]. Analogous to the polarizers used in optics, which shall split particles with orthogonal spinor states into distinct channels, they play an essential role in the entanglement detection such as the two-channel Bell inequality (BI) test [38,39]. Moreover, the polarization of the beam splitters should be adjustable, which is beyond state-of-the-art techniques of solid-state physics.

In this Letter, we propose to generate and detect a novel type of entanglement encoded in the Nambu spinor (or the electron-hole qubits) carried by quasiparticles excited in quantum Hall edge states; see Fig. 1(a). Taking advantage of the *opposite* charge carried by electrons and holes, the spinor states can be detected through a pure *charge* measurement, which successfully bypasses the need for spinor-selective beam splitters. We show that the BI test with entangled Nambu spinors can be implemented by measuring the charge-current correlation, with the polarization directions of the effective detectors on both sides being adjusted by a voltage gate and a superconductor coupled to the edge states; see Fig. 1. Given that the main ingredients of our proposal have all been realized experimentally, the observation of a considerable violation of the BI can be expected to come into reach.

The existence of the Fermi sea at zero temperature allows one to redefine it as the vacuum $|0\rangle$ of electronlike and holelike excitations. The Nambu spinor is defined by the superposition

$$|\mathbf{n}\rangle = \cos\frac{\theta}{2}|\mathbf{e}\rangle + e^{i\varphi}\sin\frac{\theta}{2}|\mathbf{h}\rangle, \tag{1}$$

where $|\mathbf{e}(\mathbf{h})\rangle = \gamma^{\dagger}_{e(h)}|0\rangle$ is the electron (hole) state created by the quasiparticle operator $\gamma^{\dagger}_{e(h)}$. It can be visualized by

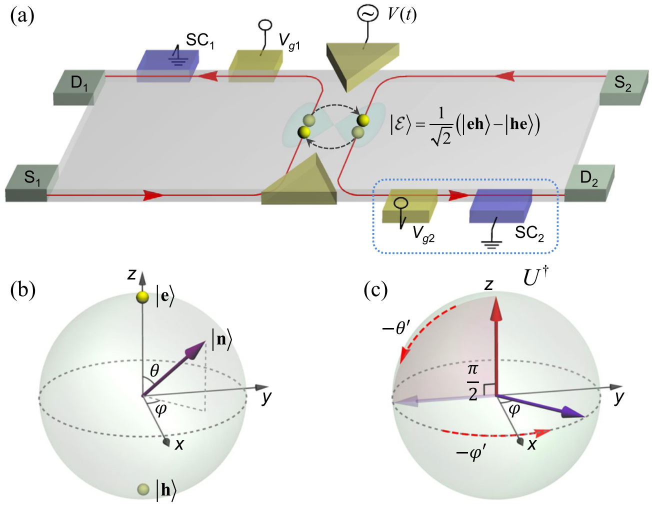

FIG. 1. (a) Proposed setup constructed on the single chiral edge state (arrowed lines) in the integer quantum Hall regime. Quasiparticle entanglement is generated in the central region (hourglass area) by a periodic electrical potential $V(t)$. Two sources ($S_{1,2}$) and two drains ($D_{1,2}$) are all grounded. A grounded superconductor ($\mathrm{SC}_{1,2}$) and a voltage gate ($V_{g1,2}$) are coupled to the outgoing channel on each side. (b) Representation of the Nambu spinor on the Bloch sphere. The north and south poles correspond to the electron ($|\mathbf{e}\rangle$) and hole ($|\mathbf{h}\rangle$) states, respectively. (c) The actions of $\mathrm{SC}_{1,2}$ and $V_{g1,2}$ inside the dashed box in (a) induce an effective rotation of the Nambu spinor.

the unit vector $\mathbf{n} = (\sin\theta\cos\varphi, \sin\theta\sin\varphi, \cos\theta)$ on the Bloch sphere as shown in Fig. 1(b). In particular, the north and south poles represent the classical states $|\mathbf{e}\rangle \Leftrightarrow |\uparrow\rangle$ and $|\mathbf{h}\rangle \Leftrightarrow |\downarrow\rangle$, which resemble the conventional spin-up and spin-down states, respectively. The advantageous feature of the Nambu spinor $|\mathbf{n}\rangle$ is that the electron and hole components have opposite charge, so that the expectation value of the pseudospin τ_z (with $\tau_{x,y,z}$ the Pauli matrices in Nambu space) is given by $\langle\tau_z\rangle = \cos\theta = \langle Q\rangle/e$, the average charge $\langle Q\rangle$ of the quasiparticle divided by the elementary charge e. As a result, the detection of the Nambu spinor along the z direction is equivalent to measuring the charge that can be implemented *locally* without a beam splitter, in stark contrast to the cases of the spin and orbital states [13–28]. Moreover, a perfect detection rate is also assured thanks to the chiral edge states being immune to backscattering.

Next, we show that probing the Nambu spinor along a general direction $\mathbf{n}$, a precondition for the entanglement detection, can be achieved by coupling the edge state to a voltage gate and a grounded superconductor [Fig. 1(a)]. These physical elements induce two effective rotations of the Nambu spinor [Fig. 1(c)], with (i) the gate voltage V_g generating a rotation $U_G(\varphi') = \exp\{-i\varphi'\tau_z/2\}$ about the z axis. This is owed to the opposite phase accumulated by the electron and hole with magnitude $\varphi' = -2eV_gL_g/(\hbar v)$ given by the length L_g of the gated region and the velocity v of the edge state. And (ii), the superconductor causes Andreev reflection [40,41] between electrons and holes and introduces the other rotation $U_S(\theta') = \exp\{-i\theta'\tau_x/2\}$ about the x axis by an angle $\theta' = 2\Delta L_s/(\hbar v)$ determined by the length L_s and the effective pair potential Δ induced by the superconductor [42]. Very recently, such coherent electron-hole conversion in the chiral edge states has been implemented in several experiments [43–47]. The detection of the Nambu spinor along the polarization direction $\mathbf{n}$ means that the initial states $|\pm\mathbf{n}\rangle$ should yield the expectation values of ± 1 or, explicitly, $\langle\pm\mathbf{n}|U^\dagger\tau_z U|\pm\mathbf{n}\rangle = \pm 1$ with $U = U_S(\theta')U_G(\varphi')$ the combined rotational operation. Given the direction of $\mathbf{n}$, this requires rotation angles $\theta' = -\theta$ and $\varphi' = -\varphi - \pi/2$, which can be implemented by proper tuning of V_g and Δ as shown in Fig. 1(c).

The bipartite entanglement of the Nambu spinor takes the form of

$$|\mathcal{E}\rangle = \frac{1}{\sqrt{2}}(|\mathbf{eh}\rangle - |\mathbf{he}\rangle), \tag{2}$$

which resembles the spin-singlet state $|\mathcal{E}\rangle \Leftrightarrow (|\uparrow\downarrow\rangle - |\downarrow\uparrow\rangle)/\sqrt{2}$. We remark that the entanglement of the Nambu spinor [26,48] is entirely *different* from the previously proposed electron-hole entanglement in Refs. [18–20]. In the latter, the electrons and holes are merely physical carriers of quantum information while the qubit is still encoded in the spin or orbital degree of freedom. In contrast, here, the electron and hole components themselves constitute the qubit.

The entangled state in Eq. (2) can be prepared by the setup fabricated on the quantum Hall edge states as shown in Fig. 1(a). The main ingredients include a central point-contact structure driven by a periodic potential $V(t) = V_0 + V_1\cos\omega t$ of frequency ω, the sources S_j and drains D_j connected to the incident and outgoing channels, and a voltage gate V_{gj} and a superconductor SC_j coupled to the outgoing channels on each side ($j = 1, 2$). The many-body state of the electrons incident from S_1 and S_2 reads $|\Psi_{\mathrm{in}}\rangle = \prod_{\epsilon<0}\gamma_{1e}^{\mathrm{in}\dagger}(\epsilon)\gamma_{2e}^{\mathrm{in}\dagger}(\epsilon)|\rangle$, with $\gamma_{1e,2e}^{\mathrm{in}\dagger}(\epsilon)$ the creation operators of the incident electrons with an energy ϵ measured from the Fermi level and $|\rangle$ being the true vacuum of the electron.

Electron-hole pairs are excited around the point-contact region by absorbing energy quanta $n\hbar\omega$ from the periodic potential [49–53]. The physical process can be well described by the Floquet scattering matrix [54,55], which relates the incident ($\gamma_{1e,2e}^{\mathrm{in}}$) and outgoing electron waves ($\gamma_{1e,2e}$) through

$$\begin{pmatrix}\gamma_{1e}(\epsilon_n)\\ \gamma_{2e}(\epsilon_n)\end{pmatrix} = s(\epsilon_n, \epsilon)\begin{pmatrix}\gamma_{1e}^{\mathrm{in}}(\epsilon)\\ \gamma_{2e}^{\mathrm{in}}(\epsilon)\end{pmatrix},$$

$$s(\epsilon_n, \epsilon) = \begin{pmatrix} r(\epsilon_n, \epsilon) & t'(\epsilon_n, \epsilon)\\ t(\epsilon_n, \epsilon) & r'(\epsilon_n, \epsilon)\end{pmatrix}, \tag{3}$$

where t, t' (r, r') are the transmission (reflection) amplitudes, $\epsilon_n = \epsilon + n\hbar\omega$, and the two components of the column vector correspond to electrons on different sides. In the limit of a weak driving potential V_1, it is sufficient to consider only the static and single-photon-assistant scattering processes described by $s_0 = [r, t'; t, r']$ and $s_\pm = s(\epsilon \pm \hbar\omega, \epsilon) = [r_\pm, t'_\pm; t_\pm, r'_\pm]$, respectively. Furthermore, the potential is assumed to vary slowly such that $\omega\delta t \ll 1$ with δt the time interval that the electron spends in the central point-contact region. In this adiabatic approximation, $s_\pm$ can be expressed in terms of s_0 as $s_\pm = V_1(\partial s_0/\partial V_1)/2$ [54].

By applying the complex conjugation of the relation Eq. (3) to the incident state $|\Psi_{\text{in}}\rangle$, one can obtain the outgoing wave function to the first order in V_1, $|\Psi_{\text{out}}\rangle = |0\rangle + |\tilde{\mathcal{E}}\rangle + |\phi\rangle$, with

$$|\tilde{\mathcal{E}}\rangle = \int_{-\hbar\omega}^{0} d\epsilon [f_{12}\gamma_{1e}^\dagger(\epsilon_1)\gamma_{2h}^\dagger(-\epsilon) - f_{21}\gamma_{1h}^\dagger(-\epsilon)\gamma_{2e}^\dagger(\epsilon_1)]|0\rangle, \tag{4}$$

the nonlocally entangled state in the form of Eq. (2) composed of quasiparticles with different energies, and $|\phi\rangle = \sum_{j=1,2}\int_{-\hbar\omega}^{0} d\epsilon f_{jj}\gamma_{je}^\dagger(\epsilon_1)\gamma_{jh}^\dagger(-\epsilon)|0\rangle$ the local electron-hole pairs. The coefficients are defined by $f_{11} = r_+ r^* + t'_+ t'^*$, $f_{12} = r_+ t^* + t'_+ r'^*$, $f_{21} = t_+ r^* + r'_+ t'^*$, and $f_{22} = t_+ t^* + r'_+ r'^*$. The unitarity of s_0 assures that $|f_{12}| = |f_{21}|$ and $|f_{11}| = |f_{22}|$, which results in a maximal entanglement in Eq. (4). In the absence of V_1, the vacuum state in terms of the outgoing waves satisfies $|0\rangle = \prod_{\epsilon<0}\gamma_{1e}^\dagger(\epsilon)\gamma_{2e}^\dagger(\epsilon)|\rangle = e^{i\delta}|\Psi_{\text{in}}\rangle$, which differs from the incident state by an unimportant overall phase δ. In the derivation of the outgoing state $|\Psi_{\text{out}}\rangle$, the particle-hole transformation $\gamma_{jh}^\dagger(\epsilon) = \gamma_{je}(-\epsilon)$ has been applied to the electrons undergoing photon-assistant scattering. The transition of an electron from energy $\epsilon \in (-\hbar\omega, 0)$ below the Fermi level to $\epsilon_1 \in (0, \hbar\omega)$ above is equivalent to the creation of an electron-hole pair in the new vacuum $|0\rangle$.

The entanglement of Nambu spinors can be measured by the charge-current correlator. As discussed previously, the drain D_j together with the gate voltage V_{gj} and the superconductor SC_j comprise an effective spinor detector along the polarization direction $\mathbf{n}_j$ (cf. Fig. 1). Mathematically, this effect can be absorbed into the modified current operator in D_j as $\hat{I}_{\mathbf{n}_j}(t) = (e/h)\int\int d\epsilon d\epsilon'\, e^{(i/\hbar)(\epsilon-\epsilon')t}\gamma_j^\dagger(\epsilon)U_{\mathbf{n}_j}^\dagger\tau_z U_{\mathbf{n}_j}\gamma_j(\epsilon')$, with $\gamma_j = (\gamma_{je}, \gamma_{jh})^T$ and the rotational operator $U_{\mathbf{n}_j} = U_S(-\theta_j)U_G(-\varphi_j - \pi/2)$ specified by the unit vector $\mathbf{n}_j = (\sin\theta_j\cos\varphi_j, \sin\theta_j\sin\varphi_j, \cos\theta_j)$ [42]. Without the actions of the gate voltage and the superconductor, we have $\mathbf{n}_j = \hat{z}$ and $U_{\mathbf{n}_j} = \tau_0$ (unit operator) so that the electron and hole contribute oppositely to the charge current which naturally measures the pseudospin τ_z.

With the two sources $S_{1,2}$ being grounded, an instantaneous current is generated by the driving potential V_1. Nevertheless, the average current associated with $|\Psi_{\text{out}}\rangle$ vanishes; i.e., $\langle\hat{I}_{\mathbf{n}_j}\rangle = 0$ [56]. Despite the zero average current, the outgoing wave can give rise to finite current fluctuations. Specifically, the zero-frequency noise power between the two drains $D_{1,2}$ is defined by $\mathcal{S}(\mathbf{n}_1, \mathbf{n}_2) = 2\int_{-\infty}^{\infty} dt\langle\delta\hat{I}_{\mathbf{n}_1}(t)\delta\hat{I}_{\mathbf{n}_2}(0)\rangle$ with $\delta\hat{I}_{\mathbf{n}_j}(t) = \hat{I}_{\mathbf{n}_j}(t) - \langle\hat{I}_{\mathbf{n}_j}\rangle$. It turns out that only $|\tilde{\mathcal{E}}\rangle$ in $|\Psi_{\text{out}}\rangle$ contributes to the noise power, while $|\phi\rangle$ contains neutral electron-hole pairs on the same side that do not induce nonlocal correlation. Therefore, the noise power reduces to $\mathcal{S}(\mathbf{n}_1, \mathbf{n}_2) = 2\int_{-\infty}^{\infty} dt\langle\tilde{\mathcal{E}}|\hat{I}_{\mathbf{n}_1}(t)\hat{I}_{\mathbf{n}_2}(0)|\tilde{\mathcal{E}}\rangle$ and provides a pure signature of the bipartite entanglement. A straightforward calculation yields

$$\mathcal{S}(\mathbf{n}_1, \mathbf{n}_2) = \mathcal{S}_{ee} - \mathcal{S}_{eh} - \mathcal{S}_{he} + \mathcal{S}_{hh} = \mathcal{S}_0\mathcal{P}(\mathbf{n}_1, \mathbf{n}_2), \tag{5}$$

where the noise power is proportional to the spinor correlation function $\mathcal{P}(\mathbf{n}_1, \mathbf{n}_2) = \langle\mathcal{E}|(\boldsymbol{\tau}_1\cdot\mathbf{n}_1)(\boldsymbol{\tau}_2\cdot\mathbf{n}_2)|\mathcal{E}\rangle = -\mathbf{n}_1\cdot\mathbf{n}_2$ with the prefactor $\mathcal{S}_0 = 2e^2\omega|f_{12}|^2/\pi$ the sum of the four terms, which satisfy $\mathcal{S}_{ee} = \mathcal{S}_{hh}$, $\mathcal{S}_{eh} = \mathcal{S}_{he}$. As a result, the spinor correlation function can be measured directly by a *single* noise power. In the previous proposals based on spin and orbital entanglement, the four spinor-resolved noise powers $\mathcal{S}_{\tau\tau'}$ $(\tau, \tau' = \uparrow, \downarrow)$ needed to be measured separately and then combined properly as in Eq. (5) to arrive at the spinor correlation $\mathcal{P}(\mathbf{n}_1, \mathbf{n}_2)$ [15–23,27,28]. This is out of reach in the experiment, not only because of its complexity in practical operations, but it is also impeded by the necessity for high-quality spinor-selective beam splitters. Remarkably, the four terms of the noise power naturally appear with correct signs in Eq. (5), which greatly facilitate the entanglement detection and improve the accuracy of measurement.

The violation of the BI involves a standard criterion for the identification of quantum entanglement. We adopt the Bell-Clauser-Horne-Shimony-Holt form of the inequality [57,58],

$$\mathcal{B} = |\mathcal{P}(\mathbf{n}_1, \mathbf{n}_2) - \mathcal{P}(\mathbf{n}_1, \tilde{\mathbf{n}}_2) + \mathcal{P}(\tilde{\mathbf{n}}_1, \mathbf{n}_2) + \mathcal{P}(\tilde{\mathbf{n}}_1, \tilde{\mathbf{n}}_2)| \le 2, \tag{6}$$

which contains four spinor correlation functions along different polarization directions. Note that the correlation functions are measured by the noise power $\mathcal{S}(\mathbf{n}_1, \mathbf{n}_2)$ via the relation in Eq. (5). Specifically, the polar angle θ_j and the azimuthal angle φ_j of the spinor "polarizer" are controlled by the coupling to the superconductor and the gate voltage through $\theta_j = -2\Delta_j L_s/(\hbar v)$ and $\varphi_j = 2eV_{gj}L_g/(\hbar v) - \pi/2$, respectively, where we have assumed that the superconductors (gating regions) on the two sides are of the same length, L_s (L_g).

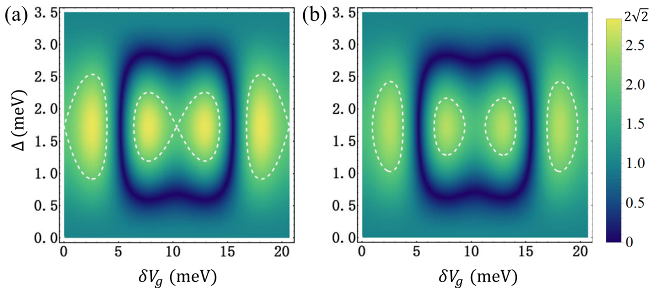

FIG. 2. Plot of $\mathcal{B}$ as a function of Δ and δV_g with (a) $\lambda = 1$ and (b) $\lambda = 0.9$. The dashed lines are the critical contours of $\mathcal{B} = 2$. The relevant parameters are set as $v = 1 \times 10^6$ m/s, $L_s = 300$ nm, and $L_g = 100$ nm.

For $\theta_1 = \theta_2 = \theta$, the violation of the BI can be tested by taking the configuration of the azimuthal angles as $\varphi_1 - \varphi_2 = \tilde{\varphi}_1 - \tilde{\varphi}_2 = \varphi_2 - \tilde{\varphi}_1 = \delta\varphi = 2e\delta V_g L_g/(\hbar v)$, which can be regulated simply by the gate voltages $V_{g1,2}$ on both sides. Assuming experimentally realizable parameters for the setup (see caption of Fig. 2), that can be achieved by modern electron-beam lithography techniques [8–12,43–47], we plot $\mathcal{B}$ as a function of Δ and δV_g in Fig. 2(a). One can see that the violation of the BI occurs in a large parameter region encircled by the critical contour $\mathcal{B} = 2$ (dashed lines). The maximal violation $\mathcal{B} = 2\sqrt{2}$ takes place when $\Delta = 1.73$ meV, and $V_{g1} - V_{g2} = \tilde{V}_{g1} - \tilde{V}_{g2} = V_{g2} - \tilde{V}_{g1} = \delta V_g = 2.59$ meV, which corresponds to $\theta = \pi/2$ and $\delta\varphi = \pi/4$, respectively (for results on more general cases with $\theta_1 \neq \theta_2$, see Supplemental Material [42]).

The detection of entanglement requires the system to preserve phase coherence. In reality, dephasing dominated by energy averaging and temperature smearing is present in the quantum Hall edge state [10,11]. Then the entanglement should be described by the density matrix $\hat{\rho} = [|\mathbf{eh}\rangle\langle\mathbf{eh}| + |\mathbf{he}\rangle\langle\mathbf{he}| - \lambda(|\mathbf{eh}\rangle\langle\mathbf{he}| + |\mathbf{he}\rangle\langle\mathbf{eh}|)]/2$ with $\lambda \in [0, 1]$ the dephasing factor which can be estimated by $\lambda \simeq e^{-(L_g+L_s)/L_\phi}$ with L_ϕ the phase coherence length. Accordingly, the crossed current correlation is evaluated by $\langle \delta\hat{I}_{\mathbf{n}_1}(t)\delta\hat{I}_{\mathbf{n}_2}(0)\rangle = \mathrm{Tr}[\hat{\rho}\delta\hat{I}_{\mathbf{n}_1}(t)\delta\hat{I}_{\mathbf{n}_2}(0)]$ and the spinor correlation function becomes $\mathcal{P}'(\mathbf{n}_1, \mathbf{n}_2) = -\cos\theta_1\cos\theta_2 - \lambda\cos(\varphi_1 - \varphi_2)\sin\theta_1\sin\theta_2$. The BI parameter $\mathcal{B}$ as a function of Δ and δV_g is plotted in Fig. 2(b). One can see that the areas of BI violation maintain, along with a certain shrinkage. The BI can be violated as long as $\lambda > 1/\sqrt{2}$, similar to the situation of the two-qubit Werner states [59–61].

Sufficiently long coherence length and two-particle interference have both been realized in mesoscopic devices constructed on quantum Hall edge states [10,11]. A visibility as high as 90% of the oscillating pattern of the quantum Hall interferometer (with a path length $\sim$4 μm) has been implemented [10], which indicates an associated value $\lambda \simeq 0.9$. Therefore, a considerable violation of the BI can be achieved with the proposed length scales L_s and L_g given in Fig. 2. Moreover, the dephasing processes that occur after the wave packet is transmitted through the voltage gate and superconducting region do not affect the entanglement detection. The reason is that the action of the random phase modulation commutes with τ_z and thus cancels out its complex conjugation in the current operator $\hat{I}_{\mathbf{n}_j}(t)$. As a result, only the lengths L_g and L_s are of importance for coherent transport, that further relaxes the constraint on the scale of the setup by L_ϕ.

We specify the experimental procedures in detail. The polarization direction $\mathbf{n}_j$ of the spinor detector can be adjusted by the gate voltage V_{gj} and the Andreev reflection at the superconductor SC_j [43–47]. It is convenient to place the four vectors $\mathbf{n}_j$, $\tilde{\mathbf{n}}_j$ in Eq. (6) to the x-y plane, i.e., $\theta_j = \pi/2$ [cf. Fig. 1(c)] and change the azimuthal angles φ_j by V_{gj}. This corresponds to an Andreev reflection with 50% probability, which can be realized by tuning the magnetic field or a large backgate [43–47]. To confirm the correct setting, one can exert a large potential V_0 at the central point contact to pinch off the connection between the edge channels on both sides. Then by imposing a small bias $V_{sj} \ll \Delta_j$ to the source S_j and measuring the current I_{dj} in the drain D_j, one can verify $\theta_j = \pi/2$ by $I_{dj} = 0$ [42].

The quantitative relation between the azimuthal angle φ_j and the gate voltage V_{gj} should be established as well. To implement this, four auxiliary point contacts $G_{1\text{–}4}$ are fabricated to construct a Mach-Zehnder interferometer on each side [10,11]; see Fig. S.2 in the Supplemental Material [42]. The whole setup is still pinched off at the center by a large V_0. By fitting the oscillation pattern modulated by V_{gj} one can obtain the angle φ_j as its function. A linear dependence $\varphi_j \propto V_{gj}$ usually holds in the regime of interest [10,11], which facilitates the calibration of φ_j.

The prefactor $\mathcal{S}_0$ in Eq. (5) should be probed so as to normalize the spinor correlation function. Note that without the superconductor, the noise power equals $\mathcal{S}(\hat{z}, \hat{z}) = -\mathcal{S}_0$. Therefore, $\mathcal{S}_0$ can be measured directly by the noise power between the two auxiliary drains $D_{3,4}$ with the auxiliary point contacts $G_{2,4}$ being pinched off [42]. In the measurement of $\mathcal{S}_0$ one first reduces V_0 to allow tunneling between the edge states on different sides and then imposes the driving potential V_1. The same setting of V_0 and V_1 should be used during the Bell measurement. With the calibration of all the parameters discussed above, the spinor correlation can be determined through $\mathcal{P}(\mathbf{n}_1, \mathbf{n}_2) = \mathcal{S}(\mathbf{n}_1, \mathbf{n}_2)/\mathcal{S}_0$. After completing these calibrations, the gate voltages at the auxiliary point contacts should be removed to separate the edge channels on opposite sides during the entanglement detection [42], and the whole setup reduces to that in Fig. 1.

One remaining point that needs clarification is the existence of several undetermined phases. They are (i) the residual phases for the azimuthal angles φ_j at $V_{gj} = 0$ accumulated during free propagation, which we denote by their difference $\gamma_1 = (\varphi_1 - \varphi_2)|_{V_{gj}=0}$, (ii) the U(1) phases of the superconducting order parameters of $SC_{1,2}$ whose difference is denoted by $\gamma_2 = \arg(\Delta_1) - \arg(\Delta_2)$, and (iii) the phase difference between the two coefficients in Eq. (4) denoted by $\gamma_3 = \arg(f_{12}) - \arg(f_{21})$. In our previous discussion, all these phases have been chosen to be zero for simplicity. We remark that these nonzero phases $\gamma_{1,2,3}$ do not affect the entanglement detection and the violation of the BI. Specifically, they only introduce an overall phase shift to the spinor correlation as $\mathcal{P}(\mathbf{n}_1, \mathbf{n}_2) = -\cos\theta_1 \cos\theta_2 - \cos(\varphi_1 - \varphi_2 + \sum_{l=1}^{3} \gamma_l) \sin\theta_1 \sin\theta_2$, which can be simply absorbed into φ_1 or φ_2. For the entanglement detection, the absolute values of $\varphi_{1,2}$ are not important, but only their differences [62].

To summarize, we propose to detect the entanglement of quasiparticles by encoding the qubit in the electron and hole components of the Nambu spinor. The effective spinor correlator can be measured directly by a single noise power function without spinor-selective beam splitters and the BI can be considerably violated. Our scheme is pertaining to condensed matter physics, where the unique many-body fermionic ground state allows for the definition of an electron-hole spinor, that has no optical counterpart. The entangled Nambu spinors can be used to explore other quantum correlation effects and may lead to interesting applications in quantum information processing.

This work was supported by the National Natural Science Foundation of China under Grants No. 12074172 (W. C.), No. 12222406 (W. C.), No. 12174182 (D. Y. X.), and No. 11804130 (W. L.), Fundamental Research Funds for the Central Universities (W. C.), the startup grant at Nanjing University (W. C.), the State Key Program for Basic Researches of China under Grant No. 2021YFA1400403 (D. Y. X.), the Excellent Programme at Nanjing University, and financial support from the Swiss National Science Foundation (SNSF) through Division II and QSIT (W. C. and G. B.).

*Corresponding author.
pchenweis@gmail.com

[1] A. Einstein, B. Podolsky, and N. Rosen, Can quantum-mechanical description of physical reality be considered complete?, Phys. Rev. **47**, 777 (1935).

[2] Erwin Schrödinger, Discussion of probability relations between separated systems, in *Mathematical Proceedings of the Cambridge Philosophical Society* (Cambridge University Press, Cambridge, England, 1935), Vol. 31, p. 555.

[3] C. H. Bennett and D. P. DiVincenzo, Quantum information and computation, Nature (London) **404**, 247 (2000).

[4] M. A. Nielsen and I. L. Chuang, *Quantum Computation and Quantum Information* (Cambridge University Press, Cambridge, England, 2000).

[5] A. K. Ekert, Quantum Cryptography Based on Bell's Theorem, Phys. Rev. Lett. **67**, 661 (1991).

[6] C. H. Bennett, G. Brassard, C. Crépeau, R. Jozsa, A. Peres, and W. K. Wootters, Teleporting an Unknown Quantum State via Dual Classical and Einstein-Podolsky-Rosen Channels, Phys. Rev. Lett. **70**, 1895 (1993).

[7] J.-W. Pan, Z.-B. Chen, C.-Y. Lu, H. Weinfurter, A. Zeilinger, and M. Żukowski, Multiphoton entanglement and interferometry, Rev. Mod. Phys. **84**, 777 (2012).

[8] M. Henny, S. Oberholzer, C. Strunk, T. Heinzel, K. Ensslin, M. Holland, and C. Schönenberger, The fermionic Hanbury Brown and Twiss experiment, Science **284**, 296 (1999).

[9] W. D. Oliver, J. Kim, R. C. Liu, and Y. Yamamoto, Hanbury Brown and Twiss-type experiment with electrons, Science **284**, 299 (1999).

[10] Y. Ji, Y. Chung, D. Sprinzak, M. Heiblum, D. Mahalu, and H. Shtrikman, An electronic Mach–Zehnder interferometer, Nature (London) **422**, 415 (2003).

[11] I. Neder, N. Ofek, Y. Chung, M. Heiblum, D. Mahalu, and V. Umansky, Interference between two indistinguishable electrons from independent sources, Nature (London) **448**, 333 (2007).

[12] E. Weisz, H. K. Choi, I. Sivan, M. Heiblum, Y. Gefen, D. Mahalu, and V. Umansky, An electronic quantum eraser, Science **344**, 1363 (2014).

[13] G. B. Lesovik, T. Martin, and G. Blatter, Electronic entanglement in the vicinity of a superconductor, Eur. Phys. J. B **24**, 287 (2001).

[14] P. Recher, E. V. Sukhorukov, and D. Loss, Andreev tunneling, Coulomb blockade, and resonant transport of nonlocal spin-entangled electrons, Phys. Rev. B **63**, 165314 (2001).

[15] S. Kawabata, Test of Bell's inequality using the spin filter effect in ferromagnetic semiconductor microstructures, J. Phys. Soc. Jpn. **70**, 1210 (2001).

[16] N. M. Chtchelkatchev, G. Blatter, G. B. Lesovik, and T. Martin, Bell inequalities and entanglement in solid-state devices, Phys. Rev. B **66**, 161320(R) (2002).

[17] P. Samuelsson, E. V. Sukhorukov, and M. Büttiker, Orbital Entanglement and Violation of Bell Inequalities in Mesoscopic Conductors, Phys. Rev. Lett. **91**, 157002 (2003).

[18] C. W. J. Beenakker, C. Emary, M. Kindermann, and J. L. van Velsen, Proposal for Production and Detection of Entangled Electron-Hole Pairs in a Degenerate Electron Gas, Phys. Rev. Lett. **91**, 147901 (2003).

[19] P. Samuelsson, E. V. Sukhorukov, and M. Büttiker, Two-Particle Aharonov-Bohm Effect and Entanglement in the Electronic Hanbury Brown–Twiss Setup, Phys. Rev. Lett. **92**, 026805 (2004).

[20] C. W. J. Beenakker, Electron-hole entanglement in the fermi sea, in *Proceedings of the International School of Physics "Enrico Fermi"* (IOS Press, Amsterdam, 2006), Vol. 162.

[21] A. V. Lebedev, G. B. Lesovik, and G. Blatter, Entanglement in a noninteracting mesoscopic structure, Phys. Rev. B **71**, 045306 (2005).

[22] P. Samuelsson and M. Büttiker, Dynamic generation of orbital quasiparticle entanglement in mesoscopic conductors, Phys. Rev. B **71**, 245317 (2005).

[23] W. Chen, R. Shen, L. Sheng, B. G. Wang, and D. Y. Xing, Electron Entanglement Detected by Quantum Spin Hall Systems, Phys. Rev. Lett. **109**, 036802 (2012).

[24] W. Chen, R. Shen, Z. D. Wang, L. Sheng, B. G. Wang, and D. Y. Xing, Quantitatively probing two-electron entanglement with a spintronic quantum eraser, Phys. Rev. B **87**, 155308 (2013).

[25] A. Schroer, B. Braunecker, A. Levy Yeyati, and P. Recher, Detection of Spin Entanglement via Spin-Charge Separation in Crossed Tomonaga-Luttinger Liquids, Phys. Rev. Lett. **113**, 266401 (2014).

[26] L. Chirolli, J. P. Baltanás, and D. Frustaglia, Chiral Majorana interference as a source of quantum entanglement, Phys. Rev. B **97**, 155416 (2018).

[27] A. Di Lorenzo and Y. V. Nazarov, Full Counting Statistics with Spin-Sensitive Detectors Reveals Spin Singlets, Phys. Rev. Lett. **94**, 210601 (2005).

[28] B. Braunecker, P. Burset, and A. Levy Yeyati, Entanglement Detection from Conductance Measurements in Carbon Nanotube Cooper Pair Splitters, Phys. Rev. Lett. **111**, 136806 (2013).

[29] L. Hofstetter, S. Csonka, J. Nygård, and C. Schöenenberger, Cooper pair splitter realized in a two-quantum-dot Y-junction, Nature (London) **461**, 960 (2009).

[30] L. G. Herrmann, F. Portier, P. Roche, A. L. Yeyati, T. Kontos, and C. Strunk, Carbon Nanotubes as Cooper-Pair Beam Splitters, Phys. Rev. Lett. **104**, 026801 (2010).

[31] J. Wei and V. Chandrasekhar, Positive noise cross-correlation in hybrid superconducting and normal-metal three-terminal devices, Nat. Phys. **6**, 494 (2010).

[32] L. Hofstetter, S. Csonka, A. Baumgartner, G. Fülöp, S. d'Hollosy, J. Nygård, and C. Schönenberger, Finite-Bias Cooper Pair Splitting, Phys. Rev. Lett. **107**, 136801 (2011).

[33] J. Schindele, A. Baumgartner, and C. Schönenberger, Near-Unity Cooper Pair Splitting Efficiency, Phys. Rev. Lett. **109**, 157002 (2012).

[34] A. Das, Y. Ronen, M. Heiblum, D. Mahalu, A. V. Kretinin, and H. Shtrikman, High-efficiency Cooper pair splitting demonstrated by two-particle conductance resonance and positive noise cross-correlation, Nat. Commun. **3**, 1165 (2012).

[35] G. Fülöp, F. Domínguez, S. d'Hollosy, A. Baumgartner, P. Makk, M. H. Madsen, V. A. Guzenko, J. Nygård, C. Schönenberger, A. Levy Yeyati, and S. Csonka, Magnetic Field Tuning and Quantum Interference in a Cooper Pair Splitter, Phys. Rev. Lett. **115**, 227003 (2015).

[36] Z. B. Tan, D. Cox, T. Nieminen, P. Lähteenmäki, D. Golubev, G. B. Lesovik, and P. J. Hakonen, Cooper Pair Splitting by Means of Graphene Quantum Dots, Phys. Rev. Lett. **114**, 096602 (2015).

[37] Zoltán Scherübl, Gergő Fülöp, Jörg Gramich, András Pályi, Christian Schönenberger, Jesper Nygård, and Szabolcs Csonka, From Cooper pair splitting to the non-local spectroscopy of a Shiba state, Phys. Rev. Research **4**, 023143 (2022).

[38] A. Aspect, P. Grangier, and G. Roger, Experimental Realization of Einstein-Podolsky-Rosen-Bohm Gedankenexperiment: A New Violation of Bell's Inequalities, Phys. Rev. Lett. **49**, 91 (1982).

[39] W. Tittel, J. Brendel, H. Zbinden, and N. Gisin, Violation of Bell Inequalities by Photons More Than 10 km Apart, Phys. Rev. Lett. **81**, 3563 (1998).

[40] J. A. M. van Ostaay, A. R. Akhmerov, and C. W. J. Beenakker, Spin-triplet supercurrent carried by quantum Hall edge states through a Josephson junction, Phys. Rev. B **83**, 195441 (2011).

[41] C. W. J. Beenakker, Annihilation of Colliding Bogoliubov Quasiparticles Reveals Their Majorana Nature, Phys. Rev. Lett. **112**, 070604 (2014).

[42] See Supplemental Material at http://link.aps.org/supplemental/10.1103/PhysRevLett.129.120507 for the derivation of the effective spinor rotation induced by the superconductor, the calculation of shot noise and the Bell inequality, and the discussion on the parameter calibration processes.

[43] P. Rickhaus, M. Weiss, L. Marot, and C. Schönenberger, Quantum Hall effect in graphene with superconducting electrodes, Nano Lett. **12**, 1942 (2012).

[44] G.-H. Lee, K.-F. Huang, D. K. Efetov, D. S. Wei, S. Hart, T. Taniguchi, K. Watanabe, A. Yacoby, and P. Kim, Inducing superconducting correlation in quantum Hall edge states, Nat. Phys. **13**, 693 (2017).

[45] L. Zhao, E. G. Arnault, A. Bondarev, A. Seredinski, T. F. Q. Larson, A. W. Draelos, H. Li, K. Watanabe, T. Taniguchi, F. Amet, H. U. Baranger, and G. Finkelstein, Interference of chiral Andreev edge states, Nat. Phys. **16**, 862 (2020).

[46] Mehdi Hatefipour, Joseph J. Cuozzo, Jesse Kanter, William Strickland, Tzu-Ming Lu, Enrico Rossi, and Javad Shabani, Induced superconducting pairing in integer quantum Hall edge states, Nano Lett. **22**, 6173 (2022).

[47] D. Wang, E. J. Telford, A. Benyamini, J. Jesudasan, P. Raychaudhuri, K. Watanabe, T. Taniguchi, J. Hone, C. R. Dean, and A. N. Pasupathy, Andreev reflection in NbN/graphene junctions under large magnetic fields, Nano Lett. **21**, 8229 (2021).

[48] G. Strübi, W. Belzig, M.-S. Choi, and C. Bruder, Interferometric and Noise Signatures of Majorana Fermion Edge States in Transport Experiments, Phys. Rev. Lett. **107**, 136403 (2011).

[49] G. Fève, A. Mahé, J.-M. Berroir, T. Kontos, B. Placais, D. C. Glattli, A. Cavanna, B. Etienne, and Y. Jin, An on-demand coherent single-electron source, Science **316**, 1169 (2007).

[50] N. M. Gabor, Z. Zhong, K. Bosnick, P. Park, and P. L. McEuen, Extremely efficient multiple electron-hole pair generation in carbon nanotube photodiodes, Science **325**, 1367 (2009).

[51] M. Vanević, J. Gabelli, W. Belzig, and B. Reulet, Electron and electron-hole quasiparticle states in a driven quantum contact, Phys. Rev. B **93**, 041416(R) (2016).

[52] J. Dubois, T. Jullien, F. Portier, A. Cavanna, Y. Jin, P. Wegscheider, W. Roulleau, and D. C. Glattli, Minimal-excitation states for electron quantum optics using levitons, Nature (London) **502**, 659 (2013).

[53] R. Bisognin, A. Marguerite, B. Roussel, M. Kumar, C. Cabart, C. Chapdelaine, A. Mohammad-Djafari, J.-M. Berroir, E. Bocquillon, B. Plaçais, A. Cavanna, U. Gennser, Y. Jin, P. Degiovanni, and G. Fève, Quantum tomography of electrical currents, Nat. Commun. **10**, 3379 (2019).

[54] M. Moskalets and M. Büttiker, Dissipation and noise in adiabatic quantum pumps, Phys. Rev. B **66**, 035306 (2002).

[55] Michael V Moskalets, *Scattering Matrix Approach to Non-Stationary Quantum Transport* (World Scientific, Singapore, 2011).

[56] Note that the electrons and holes in $|\phi\rangle$ come up in pairs and counteract each other; furthermore, the current contribution of the nonlocal entangled state $|\tilde{\mathcal{E}}\rangle$ is calculated by the reduced density matrix $\hat{\rho}_j = |f_{12}|^2(|\mathbf{e}\rangle_j\langle\mathbf{e}|_j + |\mathbf{h}\rangle_j\langle\mathbf{h}|_j)$, which also possesses an equal weight of electron and hole.

[57] J. S. Bell, On the Einstein Podolsky Rosen paradox, Phys. Phys. Fiz. **1**, 195 (1964).

[58] J. F. Clauser, M. A. Horne, A. Shimony, and R. A. Holt, Proposed Experiment to Test Local Hidden-Variable Theories, Phys. Rev. Lett. **23**, 880 (1969).

[59] R. F. Werner, Quantum states with Einstein-Podolsky-Rosen correlations admitting a hidden-variable model, Phys. Rev. A **40**, 4277 (1989).

[60] R. Horodecki, P. Horodecki, M. Horodecki, and K. Horodecki, Quantum entanglement, Rev. Mod. Phys. **81**, 865 (2009).

[61] N. Brunner, D. Cavalcanti, S. Pironio, V. Scarani, and S. Wehner, Bell nonlocality, Rev. Mod. Phys. **86**, 419 (2014).

[62] All these unknown phases are determined by the specific conditions of the setup; they are not subject to fluctuations and thus will not destroy the phase coherence.